Interpretations of the ATLAS diboson anomaly

CrossMark

Kingman Cheung [a,b,c], Wai-Yee Keung [d,a,*], Po-Yan Tseng [b], Tzu-Chiang Yuan [e,a]

[a] *Physics Division, National Center for Theoretical Sciences, Hsinchu, Taiwan*
[b] *Department of Physics, National Tsing Hua University, Hsinchu 300, Taiwan*
[c] *Division of Quantum Phases & Devices, School of Physics, Konkuk University, Seoul 143-701, Republic of Korea*
[d] *Department of Physics, University of Illinois at Chicago, IL 60607, USA*
[e] *Institute of Physics, Academia Sinica, Nangang, Taipei 11529, Taiwan*

A B S T R A C T

Recently, the ATLAS Collaboration recorded an interesting anomaly in diboson production with excesses at the diboson invariant mass around 2 TeV in boosted jets of all the WZ, W^+W^-, and ZZ channels. We offer a theoretical interpretation of the anomaly using a phenomenological right-handed model with extra W' and Z' bosons. Constraints from narrow total decay widths, dijet cross sections, and $W/Z + H$ production are taken into account. We also comment on a few other possibilities.

© 2015 The Authors. Published by Elsevier B.V. This is an open access article under the CC BY license (http://creativecommons.org/licenses/by/4.0/). Funded by SCOAP³.

1. Introduction

Recently, the ATLAS Collaboration [1] reported an experimental anomaly in diboson production with apparent excesses in boosted jets of the W^+W^-, $W^\pm Z$, and ZZ channels at around 2 TeV invariant mass of the boson pair.[1] It is intriguing because the excesses are all around 2 TeV. The local excesses are at 3.4, 2.6, and 2.9σ levels for WZ, W^+W^-, and ZZ channels, respectively (though the global significance of the discrepancy in the WZ channel is only 2.5σ). The experiment used the method of jet substructure to discriminate the hadronic decays of the W and Z bosons from the usual QCD dijets. The advantage is that the hadronic decays of W and Z afford much larger branching ratios for more events. However, the jet masses of the W and Z bosons have large overlaps such that the Z boson may be misinterpreted as a W boson, and vice versa. Nevertheless, we attempt to provide a logical explanation for the anomaly.

The anomaly leads to a logical explanation that there exist some exotic particles in some forms of multiplets or under some symmetries (because they have similar masses) with relatively narrow widths decaying into diboson channels. In this note, we propose a phenomenological left–right model that consists of an extra $SU(2)_R$ gauge group with (W', Z') bosons. Initially, we first perform phenomenological studies of the W' and Z' boson with

respect to the data separately. At the end, we shall give a more unified picture of the W' and Z' bosons coming from a single $SU(2)_R$ group.

The W' boson couples to the right-handed fermions with a strength g_R, which need not be the same as the weak coupling g. The W' boson can then be produced via $q\bar{q}'$ annihilation. Since the W' boson is at 2 TeV, the production is mainly via valence quarks and so we anticipate the production cross section of W'^+ is roughly two times as large as the W'^- cross section at the LHC. The W' boson can mix with the SM W boson via a mixing angle, say, $\sin\phi_w$ so that the W' boson can decay into WZ with a mixing-angle suppression and right-handed fermions. We shall show that the W' decay into WZ dominates if the mixing angle is larger than 10^{-2}. Therefore, it can explain the excess in the WZ channel without violating the leptonic cross sections [3–6] and the dijet-mass search at the LHC [7,8].

The discussion of the Z' boson follows closely that of the W' boson. It is produced via $q\bar{q}$ annihilation with a coupling strength g_R. The Z' boson mixes with the SM Z boson via another mixing angle ϕ_z, and then decays into W^+W^- to explain the excess in the W^+W^- channel. We adopt a simplified form that the Z' only couples to the right-handed fermions, though in general it couples to both left- and right-handed fermions.

There are, in general, a few important constraints that restrict the form the W' and Z' models: (i) electroweak (EW) precision measurements, (ii) leptonic decays of W' and Z', and (iii) dijet production cross sections, plus WH and ZH production that are specific to the current work. The EW precision constraints mainly come from the deviations in the properties of the observed W and

---

* Corresponding author.
E-mail address: keung@uic.edu (W.-Y. Keung).
[1] The CMS Collaboration also saw a moderate excess around 2 TeV in the boosted jets of W^+W^-, $W^\pm Z$, and ZZ [2].

Z bosons through the mixings between W and W' bosons, and between Z and Z' bosons. The measured properties of the W boson restrict the mixing angle between the W and W' boson to be $\phi_w \lesssim 1.3 \times 10^{-2}$ [9], which is the approximate size of the mixing that is required to explain the diboson anomaly. On the other hand, the constraint on the mixing angle between the Z and Z' bosons is much stronger. The updated limits for various Z' models, in which the Z' boson has direct couplings to SM particles, are of order 10^{-3}. This is somewhat smaller than the values required to explain the diboson anomaly. One possibility to relax this constraint is to employ the leptophobic Z' model, which is achievable in a number of GUT models [10]. In such a case, the constraint on the mixing angle can be relaxed to 8×10^{-3} [10], which is close to the value required to explain the diboson anomaly. Therefore, we shall employ the leptophobic Z' model in this work. Furthermore, in the leptonic decays of $W'^+ \to e^+ \nu_R$ we assume the right-handed neutrinos are heavy enough that the leptonic decays of the W' boson are also closed.

Note that we take the excess in the ZZ channel as either a fluctuation or the mis-interpretation because of the overlap between the W and Z dijets. On the theory side, it is very difficult to have a spin-1 particle to decay significantly into ZZ, e.g., the Z' boson [11,12] or a techni-rho meson. It is possible to have a spin-0 Higgs-like boson to decay into ZZ. However, we found that the production cross section for a 2 TeV Higgs-like boson via gluon fusion is too small to explain the excess in the ZZ channel. Therefore, we take the liberty to ignore the excess in the ZZ channel.

The organization of this note is as follows. In the next section, we describe the interactions of the W' and Z' bosons, and mixing with the SM W and Z bosons. In Section 3, we calculate the dijet cross sections to compare with the most updated limits from ATLAS [7] and CMS [8]. In Section 4, we calculate the cross sections of $pp \to W' \to WZ$ and $pp \to Z' \to W^+ W^-$ and compare to the ATLAS data. In Section 5, we give a more unified picture that the W' and Z' bosons come from a single $SU(2)_R$. We conclude in Section 6.

At the last stage of this work, the authors came across Ref. [13] with a similar idea, and Refs. [14,15] in the framework of strong dynamics. There are some existing constraints in literature for models with extra $SU(2)$ [16], especially the dilepton constraint from the LHC experiments. We shall consider the dilepton constraint, as well as the dijet constraint using the most recent data from the LHC.

2. Interactions of the W' and Z' bosons and their decays

2.1. The W' boson

The extra W_2 boson arises from the right-hand $SU(2)_R$. The right-handed fermions are arranged in isospin doublet, e.g., $(u_R, d_R)^T$, $(\nu_R, e_R)^T$, where ν_R is the right-handed neutrino. The interactions of the W_2 with fermions are given by

$$\mathcal{L} \supset -\frac{g_R}{\sqrt{2}} \bar{f}' \gamma_\mu P_R f \, W_2^\mu \qquad (1)$$

where $P_{L,R} = (1 \mp \gamma^5)/2$ and g_R is the coupling strength, which need not be the same as the left-handed coupling g but should be of a similar size. The W_1 and W_2 denote the interaction eigenstates, which rotate into the mass eigenstates W and W' via a mixing angle ϕ_w (W then represents the observed W boson at 80.4 GeV and the W' is the hypothetical 2 TeV boson):

$$\begin{pmatrix} W_1 \\ W_2 \end{pmatrix} = \begin{pmatrix} \cos\phi_w & -\sin\phi_w \\ \sin\phi_w & \cos\phi_w \end{pmatrix} \begin{pmatrix} W \\ W' \end{pmatrix}. \qquad (2)$$

Current EW constraints on the W–W' mixing angle mainly come from modifying the properties of the observed W boson. The measurements put a limit about 1.3×10^{-2} [9] on the mixing angle ϕ_w, which is more or less consistent with the values that we use in this study (see Fig. 4). We shall show that such a small mixing angle of order $O(10^{-2})$ is enough to explain the narrow width of the W' bump and the excess in the WZ production cross section.

On the other hand, due to the mixing with the SM W boson, the heavy W' couples to WZ with a coupling strength $(g \cos\theta_w) \sin\phi_w$, where $(g \cos\theta_w)$ is the usual coupling constant in the WWZ vertex. On the other hand, the W' couples to WH with a full tree-level strength $(g M_W) \sin\phi_w \cos^2\theta_w \frac{M_{W'}^2}{M_W^2}$.[2] Now we can write down the relevant vertices of the W' used in this work ($\cos\phi_w \simeq 1$),

$$\mathcal{V}_{W'ff'} : -\frac{g_R}{\sqrt{2}} \bar{f}' \gamma^\mu P_R f \, \epsilon_\mu(p_{W'+}) \ ,$$

$$\mathcal{V}_{W'WZ} : +g \cos\theta_w \sin\phi_w \left[(p_{W'} - p_{W-})^\beta g^{\mu\alpha} \right.$$
$$+ (p_{W-} - p_Z)^\mu g^{\alpha\beta} + (p_Z - p_{W'+})^\alpha g^{\mu\beta} \right]$$
$$\times \epsilon_\mu(p_{W'+}) \, \epsilon_\alpha(p_{W-}) \, \epsilon_\beta(p_Z) \ ,$$

$$\mathcal{V}_{W'WH} : +g M_W \sin\phi_w \left(\cos^2\theta_w \frac{M_{W'}^2}{M_W^2} \right) g^{\mu\alpha} \epsilon_\mu(p_{W'+})$$
$$\times \epsilon_\alpha(p_{W-}) \ , \qquad (3)$$

where $p_{W'+,W-,Z}$ denote the 4-momenta of the W'^+, W^-, Z bosons going into the vertex and $\epsilon(p_{W'+})$, $\epsilon(p_{W-})$, and $\epsilon(p_Z)$ denote the corresponding polarization 4-vectors.

The partial decay width for $W' \to f \bar{f}'$ is given by, in massless limit of f, f'

$$\Gamma_{W' \to f \bar{f}'} = \frac{N_f g_R^2 M_{W'}}{48\pi} \ , \qquad (4)$$

where $N_f = 3$ (1) for quarks (leptons). Here we also assume that the right-handed neutrinos are so heavy that $W'^+ \to e^+ \nu_R$ is kinematically not allowed. Therefore, the leptonic decay modes of W' are closed. The partial width into WZ is [17]

$$\Gamma_{W'+ \to W+Z}$$
$$= \sin^2\phi_w \left(\frac{g^2 \cos^2\theta_w}{192\pi} \frac{M_{W'}^5}{M_W^2 M_Z^2} \right)$$
$$\times \left[\left(1 - \frac{M_Z^2}{M_{W'}^2} - \frac{M_W^2}{M_{W'}^2} \right)^2 - \frac{4M_W^2 M_Z^2}{M_{W'}^4} \right]^{3/2}$$
$$\times \left[1 + 10 \left(\frac{M_Z^2 + M_W^2}{M_{W'}^2} \right) + \frac{M_Z^4 + M_W^4 + 10M_Z^2 M_W^2}{M_{W'}^4} \right]. \qquad (5)$$

It is easy to see that in the $W'WZ$ vertex in Eq. (3) the momentum-dependent parts will get enhancement at high energy.

---

[2] The mixing angle ϕ_w between the W and W' originates from the off-diagonal mass matrix entry, which also gives the tree-level unsuppressed coupling for W'–W–H. We found that ϕ_w scales as $M_W^2 / M_{W'}^2$ and the coupling for $W'WH$ scales as $g M_W \phi_w M_{W'}^2 / M_W^2$.
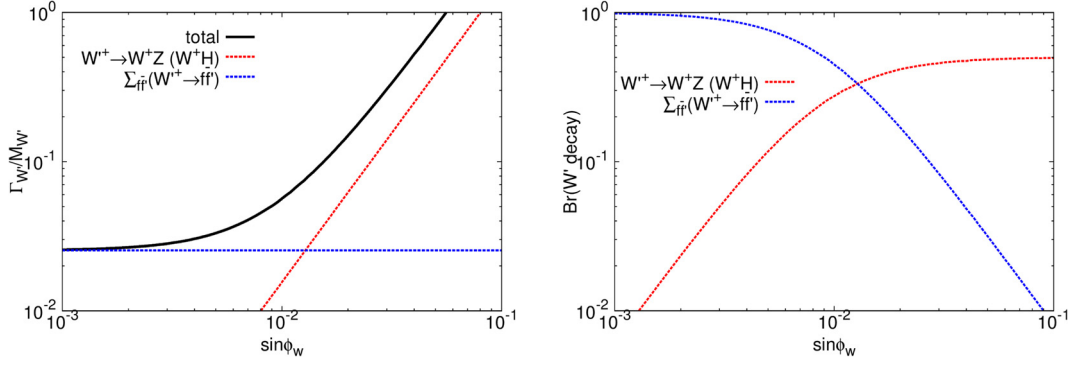
Fig. 1. (Left) Total decay width and partial widths of the 2 TeV W' boson versus the sine of the mixing angle ϕ_w. (Right) The corresponding branching ratios. Note that the W^+H appears to be the same as W^+Z in the figure. Here we take $g_R = g$. (For interpretation of the colors in this figure, the reader is referred to the web version of this article.)

Table 1

The partial widths into WZ/WH and $\sum f\bar{f}'$ and the total width of the W' boson for a few representative values of $\sin\phi_w$. We assume $\Gamma_{W'^+\to W^+Z} = \Gamma_{W'^+\to W^+H}$ and set $g_R = g$ for simplicity.

Case	$\sin\phi_w$	$\Gamma_{W'^+\to W^+Z/W^+H}$ (GeV)	$\sum_{f\bar{f}'}\Gamma_{W'^+\to f\bar{f}'}$ (GeV)	$\Gamma_{W'^+}$
1	8.901×10^{-3}	24.63	50.74	$M_{W'}/20$
2	1.549×10^{-2}	74.63	50.74	$M_{W'}/10$
3	2.370×10^{-2}	174.6	50.74	$M_{W'}/5$
4	3.148×10^{-2}	308.0	50.74	$M_{W'}/3$
5	3.908×10^{-2}	474.6	50.74	$M_{W'}/2$

Another decay channel of W' is $W' \to WH$, the partial width of which is given by

$$\Gamma_{W'^+\to W^+H} = \sin^2\phi_w \left(\frac{g^2}{192\pi} \cos^4\theta_w \frac{M_{W'}^5}{M_W^4} \right)$$
$$\times \left[\left(1 + \frac{M_W^2}{M_{W'}^2} - \frac{M_H^2}{M_{W'}^2} \right)^2 + 8\frac{M_W^2}{M_{W'}^2} \right]$$
$$\times \left[\left(1 - \frac{M_W^2}{M_{W'}^2} - \frac{M_H^2}{M_{W'}^2} \right)^2 - 4\frac{M_W^2 M_H^2}{M_{W'}^4} \right]^{1/2} . \quad (6)$$

Note that due to the Equivalence Theorem, $\Gamma(W'^+ \to W^+H) \simeq \Gamma(W'^+ \to W^+Z)$ to the leading order in $1/M_{W'}^2$.

In order to avoid a too-broad resonance structure for the W' boson we require

$$\Gamma_{\text{tot}}(W'^+) = \Gamma_{W'^+\to W^+Z} + \Gamma_{W'^+\to W^+H}$$
$$+ \sum_{f\bar{f}'=u\bar{d},c\bar{s},t\bar{b}} \Gamma_{W'^+\to f\bar{f}'} \quad (7)$$

to be less than one-tenth of the W' mass. We show in Fig. 1 the total width of the W' boson versus the sine of the mixing angle, and the corresponding branching ratios. Note that the W^+H appears to be the same as W^+Z in the figure. It is clear that the total decay width grows with $\sin\phi_w$ rapidly. Therefore, the requirement of $\Gamma_{\text{tot}}(W') \lesssim M_{W'}/10$ gives

$$\sin\phi_w \lesssim 1.5 \times 10^{-2} . \quad (8)$$

We show in Table 1 a few representative values of $\sin\phi_w$ for the partial widths into WZ or WH, and $\sum f\bar{f}'$ and the total width of the W' boson. Here we assume $g_R = g$ for simplicity. Note that the total width has only very mild dependence on g_R.

2.2. The Z' boson

We repeat the exercise for the Z' boson. The interactions of the Z_2 with the SM fermions are given by

$$\mathcal{L} \supset -\bar{f}\gamma_\mu(g_{f,r}P_R + g_{f,l}P_L)f\, Z_2^\mu . \quad (9)$$

The SM Z_1 boson mixes with Z_2 via a mixing angle ϕ_z into the mass eigenstates Z and Z':

$$\begin{pmatrix} Z_1 \\ Z_2 \end{pmatrix} = \begin{pmatrix} \cos\phi_z & -\sin\phi_z \\ \sin\phi_z & \cos\phi_z \end{pmatrix} \begin{pmatrix} Z \\ Z' \end{pmatrix} . \quad (10)$$

Unlike the W–W' mixing the EW constraints for the Z–Z' mixing angle are much stronger, because of all the precision measurements at LEP. The updated limit for various Z' models, in which the Z' boson has direct couplings to SM particles, is of order 10^{-3} [10]. This is somewhat smaller than the values required to explain the diboson anomaly. One possibility to relax this constraint is to employ the leptophobic Z' model, which is achievable in GUT models. In such a case, the constraint on the mixing angle can be relaxed to 8×10^{-3} [10], which is not far from the values required to solve the diboson anomaly. We shall therefore assume leptophobic couplings of the Z' boson. When the mixing angle is of that small size, the Z' boson has a narrow width.

The Z' boson then couples with a strength proportional to $g_{f,r/l}$ to the SM quarks, but at a strength suppressed by the mixing angle $\sin\phi_z$ to the W^+W^-. However, the Z' boson couples to ZH with a full tree-level strength for a reason similar to the W' boson. Now we can write down the relevant vertices of the Z' used in this work taking $\cos\phi_z \simeq 1$:

$$\mathcal{V}_{Z'ff} : -\bar{f}\gamma^\mu(g_{f,r}P_R + g_{f,l}P_L)f\, \epsilon_\mu(p_{Z'}) ,$$
$$\mathcal{V}_{Z'WW} : +g\cos\theta_w \sin\phi_z \left[(p_{Z'} - p_{W^+})^\beta g^{\mu\alpha} \right.$$
$$+ (p_{W^+} - p_{W^-})^\mu g^{\alpha\beta} + (p_{W^-} - p_{Z'})^\alpha g^{\mu\beta} \right]$$
$$\times \epsilon_\mu(p_{Z'})\,\epsilon_\alpha(p_{W^+})\,\epsilon_\beta(p_{W^-}) ,$$
$$\mathcal{V}_{Z'ZH} : +\frac{g}{\cos\theta_w}M_Z \sin\phi_z \left(\frac{M_{Z'}^2}{M_Z^2} \right) g^{\mu\alpha}\,\epsilon_\mu(p_{Z'})\,\epsilon_\alpha(p_Z) . \quad (11)$$

The partial widths into $f\bar{f}$, W^+W^-, and ZH are given by

$$\Gamma_{Z'\to f\bar{f}} = N_f \frac{g_{f,r}^2 + g_{f,l}^2}{24\pi} M_{Z'} ,$$
$$\Gamma_{Z'\to W^+W^-} = \sin^2\phi_z \left(\frac{g^2\cos^2\theta_w}{192\pi} \frac{M_{Z'}^5}{M_W^4} \right) \left(1 - \frac{4M_W^2}{M_{Z'}^2} \right)^{3/2}$$
$$\times \left(1 + 20\frac{M_W^2}{M_{Z'}^2} + 12\frac{M_W^4}{M_{Z'}^4} \right) ,$$
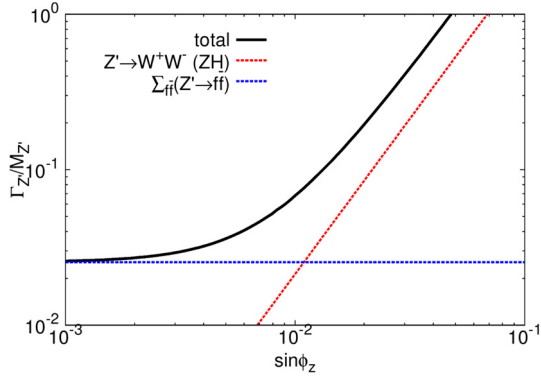
Fig. 2. Total decay width and partial widths of the 2 TeV Z' boson versus the sine of the mixing angle ϕ_z. Note that the ZH appears to be the same as W^+W^- in the figure. Here we take $g_R = g$ for simplicity. (For interpretation of the colors in this figure, the reader is referred to the web version of this article.)

$$\Gamma_{Z' \to ZH} = \sin^2 \phi_z \left(\frac{g^2 \cos^2 \theta_w}{192\pi} \frac{M_{Z'}^5}{M_W^4} \right)$$

$$\times \left[\left(1 + \frac{M_Z^2}{M_{Z'}^2} - \frac{M_H^2}{M_{Z'}^2} \right)^2 + 8 \frac{M_Z^2}{M_{Z'}^2} \right]$$

$$\times \left[\left(1 - \frac{M_Z^2}{M_{Z'}^2} - \frac{M_H^2}{M_{Z'}^2} \right)^2 - 4 \frac{M_Z^2 M_H^2}{M_{Z'}^4} \right]^{1/2}. \quad (12)$$

In the high energy limit, $\Gamma(Z' \to W^+W^-) \simeq \Gamma(Z' \to ZH)$. The total decay width of the Z' boson is obtained by summing all the above partial widths. We show the total decay width and partial widths of the Z' boson in Fig. 2. The requirement for $\Gamma_{Z'}/M_{Z'} < 0.1$ implies $\sin \phi_z \lesssim 1.5 \times 10^{-2}$.

Note that the couplings of Z_2 to quarks are model dependent (leptonic couplings are zero). We use the simplified form $g_{f,l} = 0$, $g_{f,r} = g_R T_{3,f}^{(2)}$ for the interactions according to the right-handed current $T_3^{(2)}$ as in Eq. (9). Our analysis can be generalized to any specific model by scaling the corresponding couplings.

The mixing between the Z and Z' bosons can be generated through a Higgs boson charged under both symmetries. The mixing is given by $\phi_z = C(g_R/g)(M_V/M_{V'})^2$ [18], which C can be a definite number or spanned over a range depending on the ratios of the Higgs VEVs. Given that $(M_V/M_{V'}) \sim 10^{-2}$ and $(g_R/g) \sim 0.3$–1, the mixing angle $\phi_z \sim 10^{-3}$–10^{-2}. The mixing angle that we find in this work is about 2×10^{-3}–10^{-2} and is mostly consistent with the natural value.

3. Limits from dijet production and others

Since we have assumed the leptophobic Z' model and that the right-handed neutrinos are too heavy for $W'^+ \to e^+ \nu_R$ to occur, the constraints from leptonic cross sections [3–6] can be ignored. In the following, we first consider the constraints coming from dijet production via $\sigma(W') \times B(W' \to jj)$ (and similarly for Z'). Both the ATLAS [7] and CMS [8] have searched for resonances decaying into dijets. They pose limits on the current phenomenological W' and Z' model. We calculate $pp \to W'^{\pm} \to jj$ including the width effect and show the production cross sections in Fig. 3, in which we choose $g_R = 0.6$. The acceptance factor A for each experiment is read off from the report of ATLAS and CMS. It is easy to see from both panels that when $\sin \phi_w \gtrsim 5 \times 10^{-3}$ the dijet production cross section at $M_{W'} = 2$ TeV is safe from the experimental limits. As g_R further increases, the lower limit on $\sin \phi_w$ increases, as shown in Fig. 4. Note that for $g_R \lesssim 0.5$ there is no lower limit on $\sin \phi_w$.
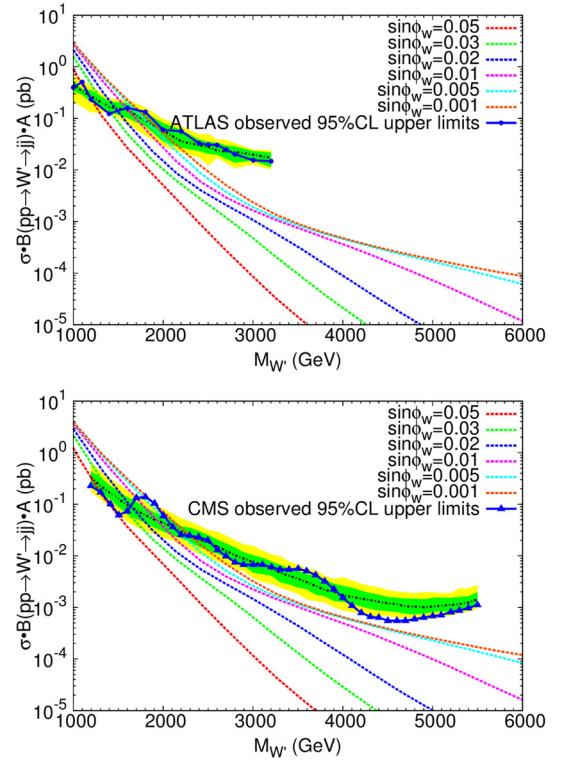
Fig. 3. Dijet production cross sections $\sigma \cdot B(pp \to W'^{\pm} \to jj) \cdot A$ versus the mass of the W' boson for a few values of $\sin \phi_w$, where A is the acceptance from the experiments. Here we take $g_R = 0.6$. The ATLAS and CMS 95% CL upper limits are also shown. (For interpretation of the colors in this figure, the reader is referred to the web version of this article.)
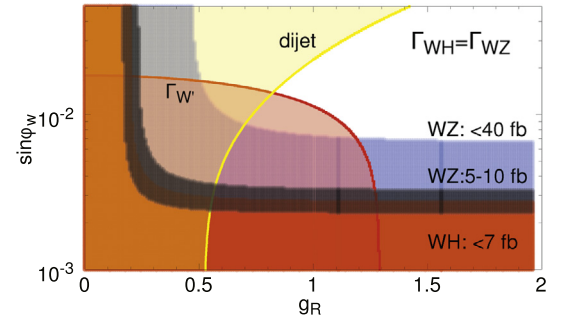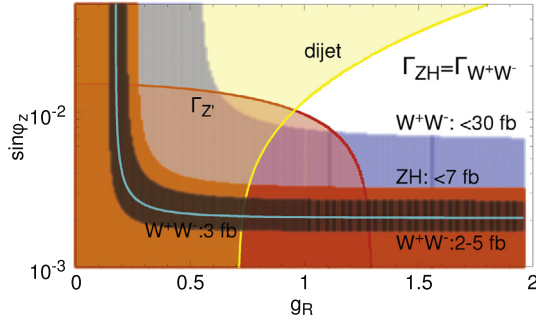

Fig. 4. The allowed parameter space in g_R versus $\sin \phi_w$ for the W' boson under the constraints: $\Gamma_{W'}/M_{W'} < 0.1$, $\sigma(W') \times B(W' \to jj) \cdot A < 60$ fb, $\sigma(W') \times B(W' \to WZ) < 40$ fb, and $\sigma(W') \times B(W' \to WH) < 7$ fb. (For interpretation of the colors in this figure, the reader is referred to the web version of this article.)

The Z' production cross sections are roughly one half of the W' for the same mass of 2 TeV. We do not expect $\sigma(Z') \times B(Z' \to jj)$ will pose any problems as long as $\phi_z \gtrsim 5 \times 10^{-3}$ for $g_R = 0.6$.

Yet, there is another constraint mentioned in Ref. [13]: $\sigma(W') \times B(W' \to WH) < 7$ fb. Both ATLAS [19] and CMS [20] searched for a resonance that decays into a W/Z boson and Higgs boson. The 95% CL on $\sigma(W'/Z') \times B(W'/Z' \to W/Z + H) \approx 5$–10 fb. As shall be seen next the required cross section for $\sigma(W') \times B(W' \to WZ)$ to explain the excess is about 6–7 fb, and a similar one for $\sigma(Z') \times B(Z' \to W^+W^-)$. It is therefore safe from the WH and ZH constraints. Finally, there was another constraint on Z' coming from a recent search on $Z' \to W^+W^-$ via the semileptonic channel of the W^+W^- decay and put an upper limit on $\sigma(Z') \times B(Z' \to W^+W^-) < 3$ fb at 95% CL [21].

We summarize in Fig. 4 the allowed parameter space of g_R versus $\sin \phi_w$ for the 2 TeV W' boson under the following constraints:

Fig. 5. The allowed parameter space in g_R versus $\sin\phi_z$ for the Z' boson under the constraints: $\Gamma_{Z'}/M_{Z'} < 0.1$, $\sigma(Z') \times B(Z' \to jj) \cdot A < 60$ fb, $\sigma(Z') \times B(Z' \to W^+W^-) < 30$ fb, $\sigma(Z') \times B(Z' \to ZH) < 7$ fb, and $\sigma(Z') \times B(Z' \to W^+W^-) < 3$ fb. (For interpretation of the colors in this figure, the reader is referred to the web version of this article.)

1. $\Gamma_{W'}/M_{W'} < 0.1$,
2. $\sigma(W') \times B(W' \to jj) \cdot A < 60$ fb [7,8],
3. $\sigma(W') \times B(W' \to WZ) < 40$ fb [1], and
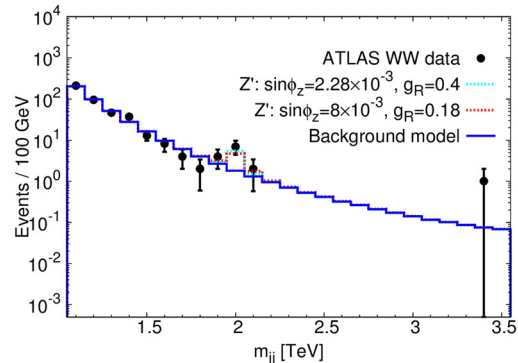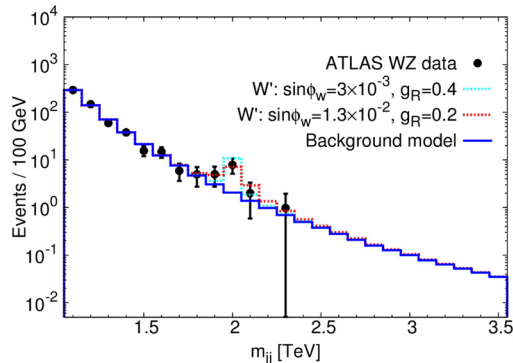4. $\sigma(W') \times B(W' \to WH) < 7$ fb [19,20].

Similarly, the allowed parameter space in g_R versus $\sin\phi_z$ for the Z' boson with the following constraints is shown in Fig. 5.

1. $\Gamma_{Z'}/M_{Z'} < 0.1$,
2. $\sigma(Z') \times B(Z' \to jj) \cdot A < 60$ fb [7,8],
3. $\sigma(Z') \times B(Z' \to W^+W^-) < 30$ fb [1],
4. $\sigma(Z') \times B(Z' \to ZH) < 7$ fb [19,20].
5. $\sigma(Z') \times B(Z' \to W^+W^-) < 3$ fb [21].

As seen in both figures the dijet cross section rules out large values of g_R while the narrow width requires $\sin\phi_w \lesssim 10^{-2}$. The overlapping region easily satisfies the WZ/WW and WH/ZH upper limits. As we shall discuss the signal cross sections in the next section, the signal cross section for $\sigma(W') \times B(W' \to WZ)$ is of order 5–10 fb while that for $\sigma(Z') \times B(Z' \to WW) \lesssim 3$ fb. We show the band of 5–10 fb cross sections onto the Fig. 4. The sweet spot is the strip obtained by overlapping the allowed region and the band of 5–10 fb. While in Fig. 5 we show the band of 2–5 fb with a cyan curve at 3 fb, because of the addition constraint $\sigma(Z') \times B(Z' \to W^+W^-) < 3$ fb via semileptonic mode [21].

4. $W' \to WZ$ and $Z' \to W^+W^-$ production

The favorable region of parameter space in g_R versus $\sin\phi_w$ is shown in Fig. 4. We can pick a point in the sweet spot to account

for the excess observed in the WZ channel. From the ATLAS report, the number of excess events is about 8–9 events around the 2 TeV peak. The selection efficiency for event topology and boson-tagging requirements is about 13% for a 2 TeV W' boson [1]. With a luminosity of 20.3 fb^{-1} it converts to $\sigma(W') \times B(W' \to WZ) \approx$ 6–7 fb (here we take the hadronic branching ratio of a W boson or a Z boson to be 0.7).

In Fig. 4, we show the band of the $\sigma(W') \times B(W' \to WZ) =$ 5–10 fb. The sweet spot is the strip obtained by overlapping the allowed region and the band of "$WZ : 5$–10 fb". Let us pick a couple of representative points: (i) $\sin\phi_w = 3 \times 10^{-3}$ and $g_R = 0.4$ (small mixing but large g_R), and (ii) $\sin\phi_w = 1.3 \times 10^{-2}$ and $g_R = 0.2$ (large mixing but small g_R). The mixing angle for the second point is at the upper limit allowed by the EW constraint. Then we calculate $\sigma(pp \to W'^{\pm} \to W^{\pm}Z)$ including the width effect, and add to the dijet background shown in the ATLAS report [1]. We show the sum of the resonance peak and the dijet background in the left panel of Fig. 6. Such a resonance contribution can explain the excess in the WZ channel. We can see that with small mixing but large g_R (the cyan histograms) the width of the 2 TeV resonance is narrower while that with large mixing but small g_R (the red histograms) is broader. Both choices can account for the data points within the uncertainties.

We repeat the exercise for the Z'. The number of excess events is about 7–8 events around the 2 TeV peak. The selection efficiency is about the same as the W'. It eventually converts to $\sigma(Z') \times B(Z' \to W^+W^-) \approx 5$–6 fb. However, due to a recent search [21] using semileptonic decay mode, the 95% CL limit on $\sigma(Z') \times B(Z' \to W^+W^-) < 3$ fb. Although there is a slight inconsistency, we pick a couple of representative points such that each gives a cross section about 3 fb: (i) $\sin\phi_z = 2.28 \times 10^{-3}$ and $g_R = 0.4$, and (ii) $\sin\phi_z = 8 \times 10^{-3}$ and $g_R = 0.18$ from the sweet spot of Fig. 5. Note that the mixing angle of the second point is at the upper limit allowed by the EW constraint. We show the sum of the resonance peak and the dijet background in the right panel of Fig. 6. Such a resonance contribution can roughly explain the excess in the W^+W^- channel within uncertainty.

5. A unified $SU(2)_1 \times SU(2)_2 \times U(1)_X$ model

Here we show that it is possible to have unified W' and Z' bosons in a model with an additional $SU(2)$ symmetry, and it will approach the models of W' and Z' that we used in Sections 2, 3 and 4. We follow closely the discussion in a couple of recent works addressing the same anomaly [22]. We start with a popular scenario based on the symmetry breaking pattern from the gauge group $SU(2)_1 \times SU(2)_2 \times U(1)_X$ (with gauge coupling

Fig. 6. Dijet invariant mass distribution for (left) $pp \to W'^{\pm} \to W^{\pm}Z$ and (right) $pp \to Z' \to W^+W^-$ with $M_{W'} = M_{Z'} = 2$ TeV. Here the finite width effect is included. A selection efficiency of 0.13, hadronic branching ratio of 0.7 for each W and Z boson, and a luminosity of 20.3 fb^{-1} are used. The dijet backgrounds are given in the ATLAS report [1].

g, g'_2, g_X respectively), which is first broken into a lower symmetry $SU(2)_1 \times U(1)_Y$ at the scale above TeV, and then broken again at the electroweak scale [23]. The intermediate symmetry is just the SM gauge group $SU(2)_L \times U(1)_Y$. The SM hypercharge convention is fixed by $Q = T_3^{(1)} + \frac{Y}{2} = T_3^{(1)} + T_3^{(2)} + \frac{Y_X}{2}$.

We choose the leptophobic version of the model such that the right-handed u_R and d_R quarks are arranged in doublet of the $SU(2)_2$ while the ν_R and e_R as singlets of the $SU(2)_2$. The assignment of $T_3^{(2)}$ and $Y_X/2$ for the right-handed fermions are

f	u_R	d_R	ν_R	e_R
$T_3^{(2)}$	$+\frac{1}{2}$	$-\frac{1}{2}$	0	0
$\frac{Y_X}{2}$	$+\frac{1}{6}$	$+\frac{1}{6}$	0	-1

The first step of symmetry breaking at TeV scale can occur via a Higgs doublet $\Phi \sim (1, 2, 1/2)$ under $SU(2)_1 \times SU(2)_2 \times U(1)_X$:

$$\Phi = \begin{pmatrix} \phi^+ \\ \phi^0 \end{pmatrix}, \qquad \langle \Phi \rangle = \frac{1}{\sqrt{2}} \begin{pmatrix} 0 \\ u \end{pmatrix}.$$

The gauge field B'_μ of the $U(1)_X$ and the W'^3_μ of the $SU(2)_2$ are rotated by angle ϕ into the B_μ of the $U(1)_Y$ and the Z' boson:

$$\begin{pmatrix} B'_\mu \\ W'^3_\mu \end{pmatrix} = \begin{pmatrix} \cos\phi & -\sin\phi \\ \sin\phi & \cos\phi \end{pmatrix} \begin{pmatrix} B_\mu \\ Z'_\mu \end{pmatrix},$$

while the second step is the usual breaking of the EW symmetry by another Higgs doublet with a VEV v. In order to obtain the coupling of the B_μ the same as the SM hypercharge $g_1 Y/2 = (e/\cos\theta_w) Y/2$ in the first step of symmetry breaking, we require

$$g_X \cos\phi = g_1, \quad g'_2 \sin\phi = g_1,$$
$$\tan\phi = \frac{g_X}{g'_2}, \quad \frac{Y_X}{2} + T_3^{(2)} = \frac{Y}{2}. \tag{13}$$

The W' and Z' bosons obtain masses as

$$M_{W'}^2 = \frac{e^2 v^2}{4\cos^2\theta_w \sin^2\phi}(x+1),$$
$$M_{Z'}^2 = \frac{e^2 v^2}{4\cos^2\theta_w \sin^2\phi \cos^2\phi}(x + \cos^4\phi), \tag{14}$$

where $x \equiv u^2/v^2$ is very large. Therefore, in leading order $M_{W'} \approx M_{Z'}$ if $\cos\phi \approx 1$. This is exactly the limit that we want to pursue, and we shall show that the couplings of the W' and Z' to fermions will approach the values that we used in the analysis.

Note that $x \sim (2\,\text{TeV}/0.1\,\text{TeV})^2 = 10^2$–$10^3$. The size of $\sin\phi$ cannot be much smaller than 0.3 given $g'_2 \lesssim 1$. In the limit of x being large, the left-handed and right-handed couplings of the W' boson to SM fermions become [22]

$$\frac{g_L^{W'ff'}}{g_R^{W'ff'}} \longrightarrow \frac{1}{x}, \quad \text{with } g_R^{W'ff'} = \frac{g'_2}{\sqrt{2}}, \tag{15}$$

which is exactly the same as the W' interaction in Eq. (1) with $g'_2 = g_R$. Similarly, in the limit of large x and small $\sin\phi$, the left-handed and right-handed couplings of the Z' boson to SM fermions become [22]

$$g_{f,l} \longrightarrow \frac{g'_2}{\cos\phi}(T_3^{(1)} - Q)\sin^2\phi$$
$$g_{f=\ell,r} \longrightarrow \frac{g'_2}{\cos\phi}(-Q\sin^2\phi)$$
$$g_{f=q,r} \longrightarrow \frac{g'_2}{\cos\phi}(T_3^{(2)} - Q\sin^2\phi)$$

Note that the leptonic couplings $g_{f=\ell,l/r}$ are suppressed by $\sin^2\phi$ and also because its $T_3^{(2)} = 0$. The left-handed couplings $g_{q,l}$ of quarks are also suppressed by $\sin^2\phi$. Therefore, only the right-handed couplings of quarks are left unsuppressed, which is close to what we used in the analysis of Z' with $g'_2 = g_R$ in previous sections. Therefore, in the limit of large x we have more or less achieved the leptophobic scenario with W' and Z' bosons having a similar mass at 2 TeV and couplings to right-handed quarks only.

6. Discussion

We have considered a phenomenological $SU(2)_R$ model that contains extra W' and Z' bosons, which mix with the SM W and Z bosons, respectively. Thus, it can induce the decays of $W' \to WZ$ and $Z' \to W^+W^-$ to explain the ATLAS anomaly in the diboson channels, while we interpreted the excess in ZZ as a fluctuation or a substantial overlap with WW and WZ. It is very difficult for a spin-1 boson to decay significantly into ZZ.

We have applied the constraints of the total width of the W' and Z' bosons, dijet cross sections, WZ and WW cross sections, and WH and ZH cross sections for the W' and Z' bosons, respectively, as well as qualitatively the EW precision constraints on the parameter space of g_R and the mixing angles ϕ_w and ϕ_z. We have found a sweet spot that satisfies all the constraints, and there exists a viable region that can explain the excess in the WZ and W^+W^- channels, respectively. The size of the mixing angle is $\phi_w, \phi_z \approx 3 \times 10^{-3}$–$10^{-2}$ and the size of the coupling $g_R \approx 0.2$–0.5.

We offer comments on our findings and other possibilities as follows.

1. The production of WZ and WW via W' and Z' bosons receives a large enhancement due to the longitudinal polarization of the W and Z boson ($\epsilon_L^\mu(W/Z) \sim p^\mu/M_{W/Z}$). If each boson-jet system (which contains 2 closely separated jets) is boosted back to the rest frame of the W/Z boson and the angle made by the jet is measured, one may be able to tell the polarization of the W/Z boson.

2. Another important channel to check is the semileptonic decays of the W and Z bosons, i.e., one boson decays leptonically while the other hadronically. Though the event rates will be lowered, the W or Z peak can be easier distinguished.

3. As we have mentioned that it is very difficult to have a spin-1 boson to decay into ZZ at tree level. There are only two effective operators describing such vertex [11], one of which may be induced by anomaly associated with the extra $U(1)$ while the other must be CP violating. The logical choice is spin-0 or spin-2. However, the production of spin-0 boson, just like the SM Higgs boson, has to go through gg fusion or WW fusion. The production cross sections are too small or the total decay width of the boson is too broad. The spin-2 boson, e.g, the graviton Kaluza–Klein state of the Randall–Sundrum model, can decay into WW and ZZ, but in the ATLAS report [1] it was shown that the production rate of the spin-2 graviton is somewhat too small to explain the anomaly.

4. Another possibility is an extended Higgs sector. It is well-known that in models with extra Higgs doublets the charged Higgs cannot couple to WZ at tree-level. It has to go beyond the doublet to e.g. triplet models. One viable triplet model is the Georgi–Machacek model [24] that contains neutral, singly-charged, and doubly-charged Higgs bosons [25]. The excess in WW channel did not distinguish between W^+W^- and $W^\pm W^\pm$. In particular, the doubly and singly charged H_5^{++} and H_5^+ can be copiously produced via vector–boson fusion for Higgs-boson mass at 2 TeV, but the width of the bosons are too broad to be consistent [26].

5. Another alternative is the strong dynamics [15], e.g., technicolor models. For example, a neutral ρ_{TC}^0 of 2 TeV can decay into $W^+ W^-$ while a charged $\rho_{TC}^\pm$ of 2 TeV can decay into $W^\pm Z$.

Acknowledgements

References

[1] G. Aad, et al., ATLAS Collaboration, arXiv:1506.00962 [hep-ex].
[2] V. Khachatryan, et al., CMS Collaboration, J. High Energy Phys. 1408 (2014) 173, arXiv:1405.1994 [hep-ex].
[3] G. Aad, et al., ATLAS Collaboration, J. High Energy Phys. 1409 (2014) 037, arXiv:1407.7494 [hep-ex].
[4] V. Khachatryan, et al., CMS Collaboration, Phys. Rev. D 91 (9) (2015) 092005, arXiv:1408.2745 [hep-ex].
[5] G. Aad, et al., ATLAS Collaboration, Phys. Rev. D 90 (5) (2014) 052005, arXiv:1405.4123 [hep-ex].
[6] V. Khachatryan, et al., CMS Collaboration, J. High Energy Phys. 1504 (2015) 025, arXiv:1412.6302 [hep-ex].
[7] G. Aad, et al., ATLAS Collaboration, Phys. Rev. D 91 (5) (2015) 052007, arXiv:1407.1376 [hep-ex].
[8] V. Khachatryan, et al., CMS Collaboration, Phys. Rev. D 91 (5) (2015) 052009, arXiv:1501.04198 [hep-ex].
[9] K.A. Olive, et al., Particle Data Group, Chin. Phys. C 38 (2014) 090001. See the section of W' in *The Review of Particle Physics*.
[10] J. Erler, P. Langacker, S. Munir, E. Rojas, J. High Energy Phys. 0908 (2009) 017, arXiv:0906.2435 [hep-ph].
[11] W.Y. Keung, I. Low, J. Shu, Phys. Rev. Lett. 101 (2008) 091802, arXiv:0806.2864 [hep-ph].
[12] T. Modak, D. Sahoo, R. Sinha, H.Y. Cheng, T.C. Yuan, arXiv:1408.5665 [hep-ph].
[13] J. Hisano, N. Nagata, Y. Omura, arXiv:1506.03931 [hep-ph].
[14] H.S. Fukano, M. Kurachi, S. Matsuzaki, K. Terashi, K. Yamawaki, arXiv:1506.03751 [hep-ph].
[15] D.B. Franzosi, M.T. Frandsen, F. Sannino, arXiv:1506.04392 [hep-ph].
[16] S. Patra, F.S. Queiroz, W. Rodejohann, arXiv:1506.03456 [hep-ph];
Q.H. Cao, Z. Li, J.H. Yu, C.P. Yuan, Phys. Rev. D 86 (2012) 095010, arXiv:1205.3769 [hep-ph].
[17] G. Altarelli, B. Mele, M. Ruiz-Altaba, Z. Phys. C 45 (1989) 109;
G. Altarelli, B. Mele, M. Ruiz-Altaba, Z. Phys. C 47 (1990) 676.
[18] P. Langacker, M.x. Luo, Phys. Rev. D 45 (1992) 278.
[19] G. Aad, et al., ATLAS Collaboration, arXiv:1503.08089 [hep-ex].
[20] V. Khachatryan, et al., CMS Collaboration, arXiv:1506.01443 [hep-ex].
[21] V. Khachatryan, et al., CMS Collaboration, J. High Energy Phys. 1408 (2014) 174, arXiv:1405.3447 [hep-ex].
[22] Q.H. Cao, B. Yan, D.M. Zhang, arXiv:1507.00268 [hep-ph];
Y. Gao, T. Ghosh, K. Sinha, J.H. Yu, arXiv:1506.07511 [hep-ph].
[23] V. Barger, W.Y. Keung, C.T. Yu, Phys. Rev. D 81 (2010) 113009, arXiv:1002.1048 [hep-ph].
[24] H. Georgi, M. Machacek, Nucl. Phys. B 262 (1985) 463.
[25] C.W. Chiang, T. Nomura, K. Tsumura, Phys. Rev. D 85 (2012) 095023, arXiv:1202.2014 [hep-ph].
[26] H. Logan, M. Zaro, Recommendations for the interpretation of LHC searches for H_5^0, $H_5^\pm$, and $H_5^{\pm\pm}$ in vector boson fusion with decays to vector boson pairs, LHCHXSWG-INT-2015-002.